Transition and Turbulent Boundary Layers

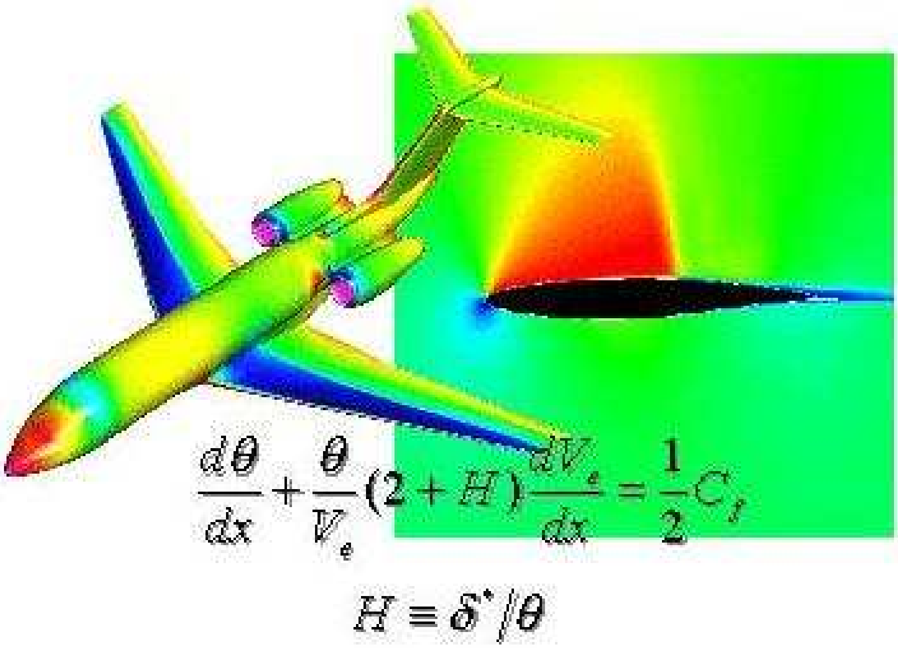

AA200b

Lecture 9

February 3, 2005

Turbulent Flows

So far we have discussed viscous flows in boundary layers that are *laminar*. By that we meant that the time derivatives in the Navier-Stokes equations could be neglected altogether, and the flows could be considered to be *steady*.

The question in nature is one of *stability*. What would happen to the boundary layer if a small disturbance, say a small eddy or a mosquito flying by, was introduced? Would the disturbance be damped out? Would the disturbance be amplified?

For low Reynolds numbers (typically Re $< 3 \times 10^5$), and for a flat plate at zero pressure gradient, the disturbances are *damped* and the flow tends to remain laminar.

For higher Reynolds numbers, disturbances tend to be amplified, leading to instability and to flows that are time dependent. These flows are said to be *tubulent* and they are nearly impossible to compute analytically, except for some very simple cases.

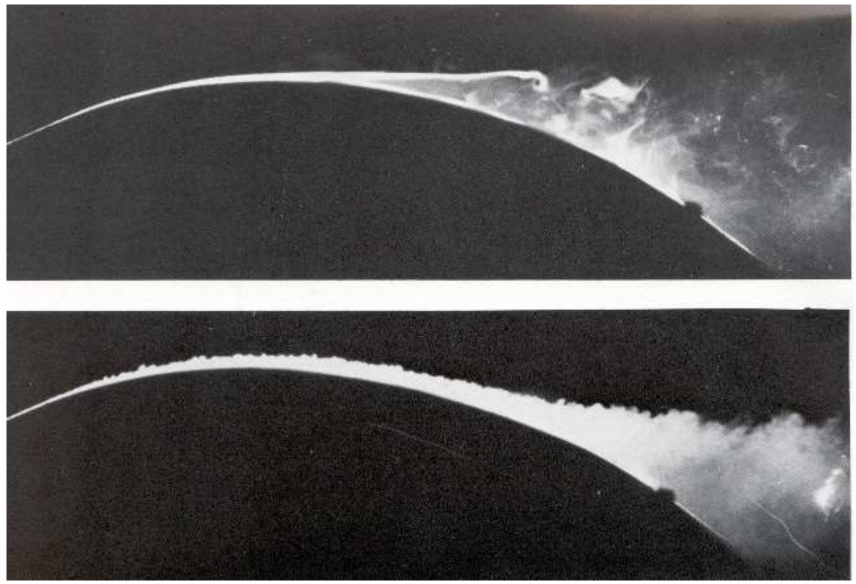

Figure 1: Laminar and Turbulent Boundary Layers

Reynolds Averaging

The most common procedure used to look at turbulent flows is called *Reynolds Averaging*. Instead of looking at the details of the unsteady turbulent flow, we look at the flow for a long period of time and concern ourselves with the *averaged* results from these observations. In this context, we define the *time average* of $u(x, y, t)$ as

$$\overline{u}(x, y) \equiv \lim_{T\to\infty} \frac{1}{T} \int_{t_0}^{t_0+T} u(x, y, t)dt. \quad (1)$$

We can now decompose the time accurate flow solution into an average and a fluctuation, $u'(x, y, t)$ as

$$u(x, y, t) = \overline{u}(x, y) + u'(x, y, t). \quad (2)$$

If we apply this time averaging process to the complete Navier-Stokes equations, and making use of the following identities for $a(x, y, t)$ and $b(x, y, t)$

$$\begin{aligned}\overline{a+b} &= \overline{a}+\overline{b}\\ \overline{a'} &= 0\\ \overline{\frac{\partial a}{\partial x}} &= \frac{\partial \overline{a}}{\partial x}\\ \overline{\overline{a}b} &= \overline{a}\overline{b},\end{aligned}$$

we obtain the result that the continuity equation is the same we had previously, but applied to the time averaged values of the velocity field

$$\frac{\partial \overline{u}}{\partial x}+\frac{\partial \overline{v}}{\partial y}=0. \tag{3}$$

The momentum equations are a little bit more complicated (see Wilcox, *Turbulence Modelling for CFD* for more details), but they effectively reduce to

$$\rho\left(\overline{u}\frac{\partial\overline{u}}{\partial x}+\overline{v}\frac{\partial\overline{u}}{\partial y}\right) = -\frac{\partial\overline{p}}{\partial x}+\frac{\partial}{\partial x}\left(\mu\frac{\partial\overline{u}}{\partial x}-\rho\overline{u'^2}\right)+\frac{\partial}{\partial y}\left(\mu\frac{\partial\overline{u}}{\partial y}-\rho\overline{u'v'}\right) \quad (4)$$

$$\rho\left(\overline{u}\frac{\partial\overline{v}}{\partial x}+\overline{v}\frac{\partial\overline{v}}{\partial y}\right) = -\frac{\partial\overline{p}}{\partial y}+\frac{\partial}{\partial x}\left(\mu\frac{\partial\overline{v}}{\partial x}-\rho\overline{u'v'}\right)+\frac{\partial}{\partial y}\left(\mu\frac{\partial\overline{v}}{\partial y}-\rho\overline{v'^2}\right)$$

These are the *time-averaged Navier-Stokes equations*. These are also sometimes called the *Reynolds-Averaged Navier-Stokes equations, RANS*. Everything looks similar to the original Navier-Stokes equations except for the terms $-\rho\overline{V_i'V_j'}$ which is usually called the *Reynolds or turbulent stress*. Unfortunately, we have three equations and six unknowns $(\overline{u},\overline{v},\overline{p},-\rho\overline{V_i'V_j'})$: we have lost information in the process of time-averaging and we must make it up somehow. It is typical to create mathematical relationships between $-\rho\overline{V_i'V_j'}$ and the values of the mean flow with what are called *turbulence* *models*. These are varied and quite involved and are the subject of complete courses here at Stanford. We will not discuss them in any more detail.

The effect of the Reynolds averaging procedure can be graphically seen in the Figure below. The first image shows the instantaneous velocity profiles at the same location along a flat plate boundary layer at 17 different instants. The profiles are shown with a series of staggered origins. In the second image, all of these velocity profiles are superimposed and then averaged to extract the view of the problem that is represented by the RANS equations.

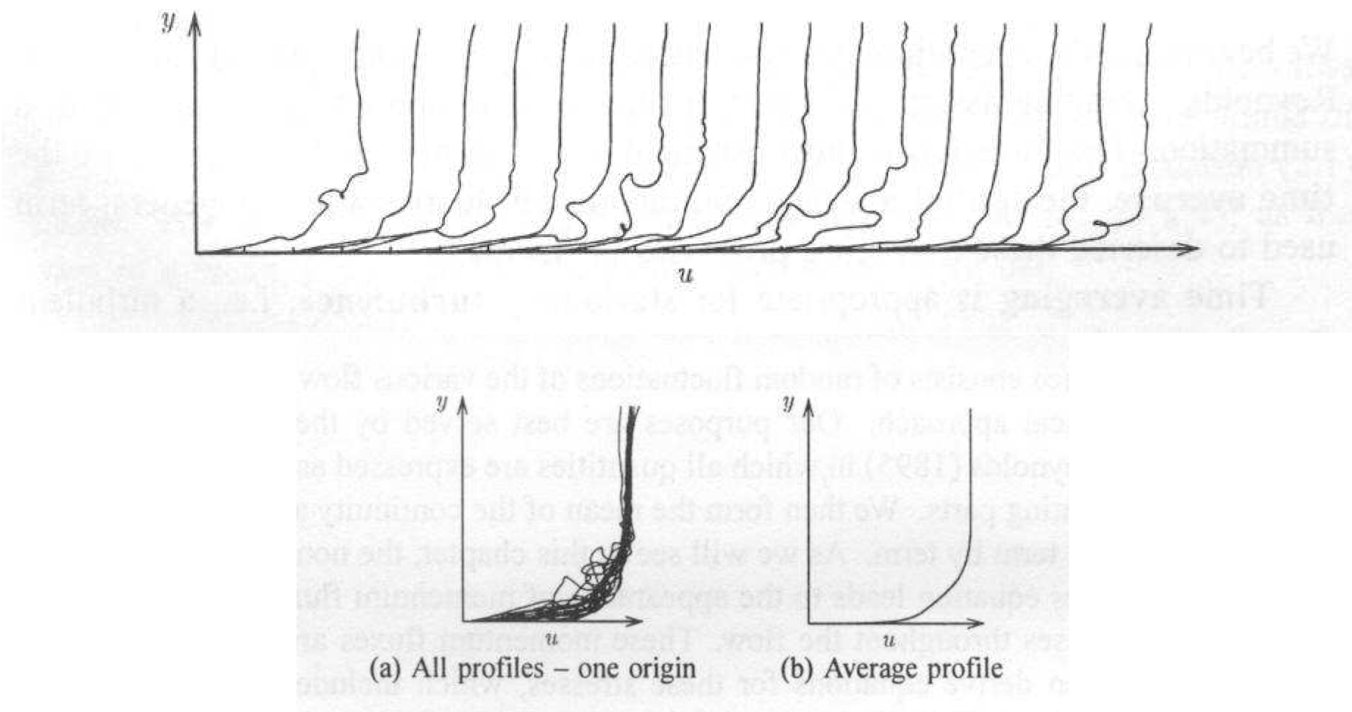

Figure 2: Instantaneous and Averaged Velocity Profiles in a Zero Pressure Gradient Boundary Layer

If we assume (as we did in the derivation of the boundary layer equations) that the characteristic length in the $y-$direction is much smaller than that in the $x-$direction, we can modify these time-averaged equations to obtain the *time-averaged boundary layer equations*

$$\begin{aligned} \rho\overline{u}\frac{\partial\overline{u}}{\partial x} + \rho\overline{v}\frac{\partial\overline{u}}{\partial y} &= -\frac{\partial\overline{p}}{\partial x} + \frac{\partial}{\partial y}\left(\mu\frac{\partial\overline{u}}{\partial y} - \rho\overline{u'v'}\right) \\ \frac{\partial\overline{p}}{\partial y} &= \frac{\partial}{\partial y}\left(\mu\frac{\partial\overline{v}}{\partial y} - \rho\overline{v'^2}\right) \end{aligned} \tag{5}$$

where we have kept terms in the $y-$momentum equation since the Reynolds stresses are all of comparable magnitude. This equation can no longer be neglected altogether as we had done for laminar flows. However, because the boundary layer is extremely thin for high Reynolds numbers, we can still take the pressure in this equation to be the *outer* inviscid pressure distribution.

Thus, the boundary layer idea is as valid in turbulent flow as it is in laminar flow. The main difference is in the order of magnitude of the terms neglected, which is $(\delta/L)^2$ in laminar flows and only (δ/L) in turbulent flows.

Transition in Two Dimensions

The natural process that leads to the instability of boundary layers is called *transition*. Because it deals with a variety of instabilities of very nonlinear equations, its study is not straightforward. We will briefly explain the most important mechanisms for transition and the factors that affect it below. This is by no means meant to be a comprehensive treatment of the topic of transition.

In purely two-dimensional flows one can perform a linear stability analysis (valid for small disturbances only) that leads to very interesting conclusions. The linear stability analysis requires the solution of the Orr-Sommerfeld equation and the calculation of amplification factors as functions of both the Reynolds number of the flow and the frequency of the disturbances. As you can see in the following figure, below a critical Reynolds number, all disturbances, regardless of their frequency, are damped, and no natural transition occurs. At higher Reynolds numbers than that value, there is always a frequency that is amplified most rapidly. If any of the unstable frequencies are present in the disturbance, the boundary layer will naturally become turbulent.

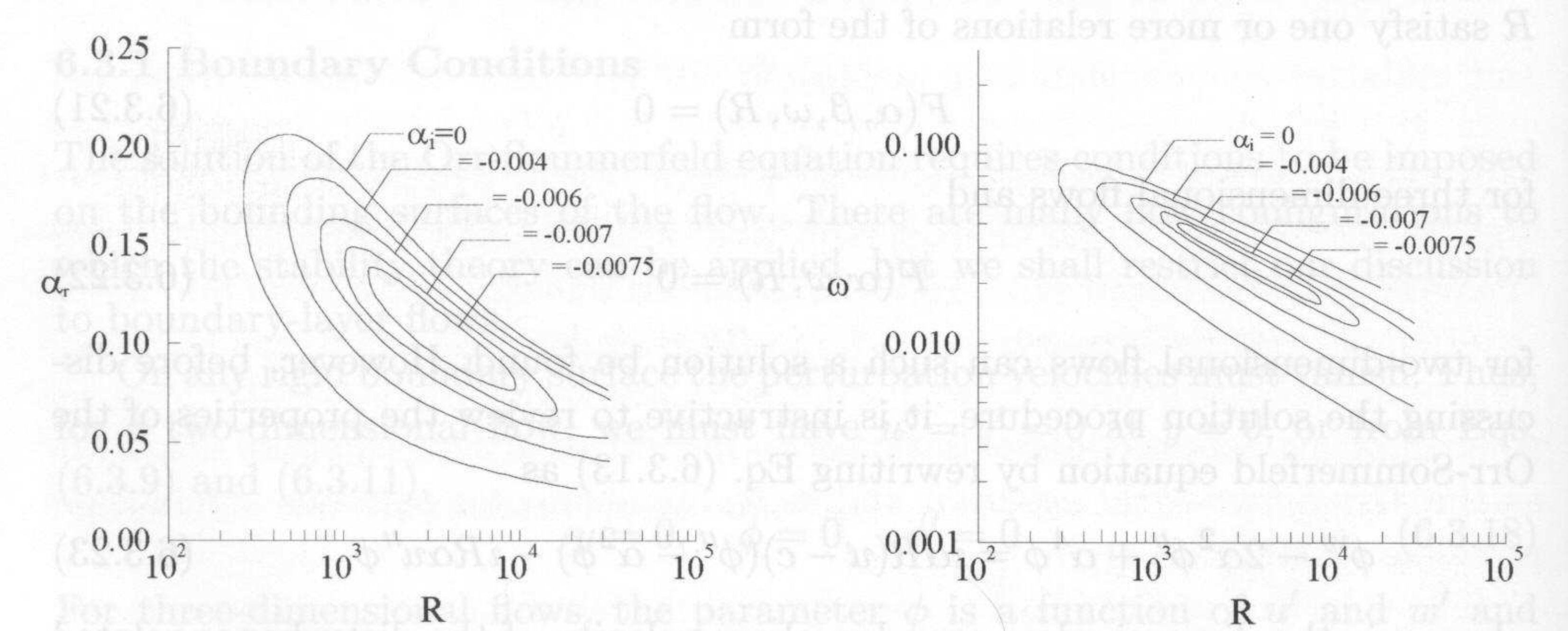

Figure 3: Amplification Factors for e^n Method

Transition in Three Dimensions

If the flow is truly three-dimensional, such as in flows over sweptback wings, the transition line is usually determined by physical phenomena that are quite different from the linear amplification process described by the Orr-Sommerfeld equation. In fact, a different phenomenon takes over altogether. We call this phenomenon *Crossflow Instability*. All of the tools that are usually developed for two-dimensional flows do not work well in three dimensions without extensive corrections because it is inflection points in the velocity distribution in the crossflow that become the dominant effect.

Factors Affecting Transition

Even with procedures developed to understand and predict transition, many variables influence the location of the transition region. Just to mention a few:

1. Freestream turbulence and noise.

2. Pressure gradients.

3. Heat transfer.

4. Suction/blowing.

5. Surface roughness and curvature.

Empirical Correlations

For imcompressible flows without heat transfer, Michel examined a variety of data (in two dimensions) and concluded that, for airfoil-type applications, transition should be expected when

$$\mathrm{Re}_\theta > 1.174\left(1 + \frac{22,400}{\mathrm{Re}_x}\right)\mathrm{Re}_x^{0.46}. \tag{6}$$

In some cases, particularly in low Reynolds number flows, separation (in the form of a separation bubble that we have already seen in class) occurs, and this is instead assumed to be the transition point for the boundary layer.

Another very popular method for transition prediction in two-dimensional, airfoil-type applications is the e^n method. This method uses the results of the Orr-Sommerfeld equation (linear stability theory) and tracks the frequency that is amplified the fastest and then sets the transition location at the point where the initial disturbance would have been amplified by a factor e^n, where n is a chosen constant that depends on the type of problem. Typically, $n = 9$, which means that transition is assumed to have occured when an initial disturbance has grown by a factor of about $8,000$. This method can be made to take pressure gradients into account and is the baseline transition mechanism in XFOIL.

Note that the n factor should be changed depending on the type of applications that we are interested in. Typically, $n_{crit} = 12 - 14$ for high performance sailplanes, 11-13 for motorgliders, 10-12 for a clean wind tunnel, and can be as low as 4-8 for a dirty wind tunnel.

Velocity Profile Fitting: Turbulent Boundary Layers

As in the Pohlhausen method, many methods for calculating turbulent boundary layers are based on an asumed parametric form of the velocity profile, $u(y)$. At first glance, it may seem that the Pohlhausen method could be used itself in turbulent flows. However, the growth of a turbulent boundary layer is not predicted accurately with the Pohlhausen method. Why? Because the assumed form of the velocity profile is far from accurately describing the true turbulent boundary layer: a simple polynomial is no longer sufficient to describe the velocity profile.

If one looks in a bit more detail at the structure of a turbulent boundary layer (see the Figure below), we see that there are more or less three distinct regions within the boundary layer:

1. *Outer Layer*: relatively sensitive to the external flow properties.

2. *Inner Layer*: turbulent mixing is the dominant influence.

3. *Laminar Sublayer*: closest to the surface, in which, because the no-slip condition forces the fluctuating velocity components to zero at the wall, the turbulent stresses are negligible compared to $\frac{\partial u}{\partial y}$.

As shown in the figure, there is a gradual transition between the laminar sublayer and the inner layer which is often called the *buffer region*. Notice that the log-log plot greatly exaggerates the extent of the laminar sublayer and the inner layer: the outer layer accounts for 80-90% of the actual boundary layer thickness.

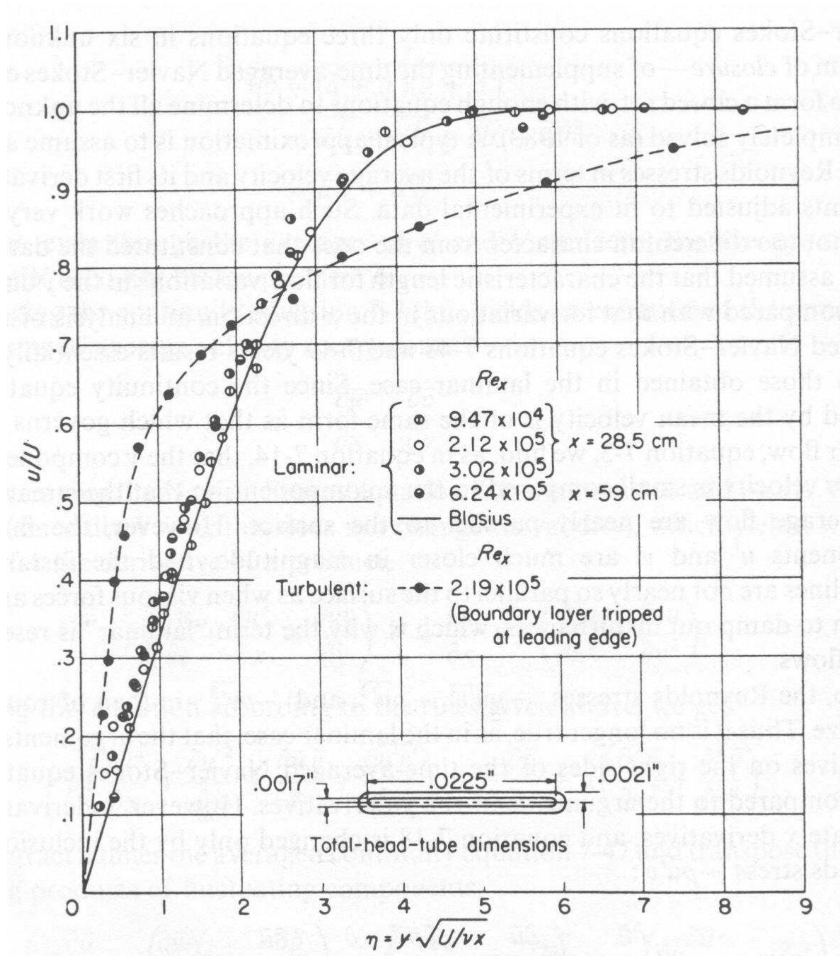

Figure 4: Laminar and Turbulent Boundary Layer Profiles

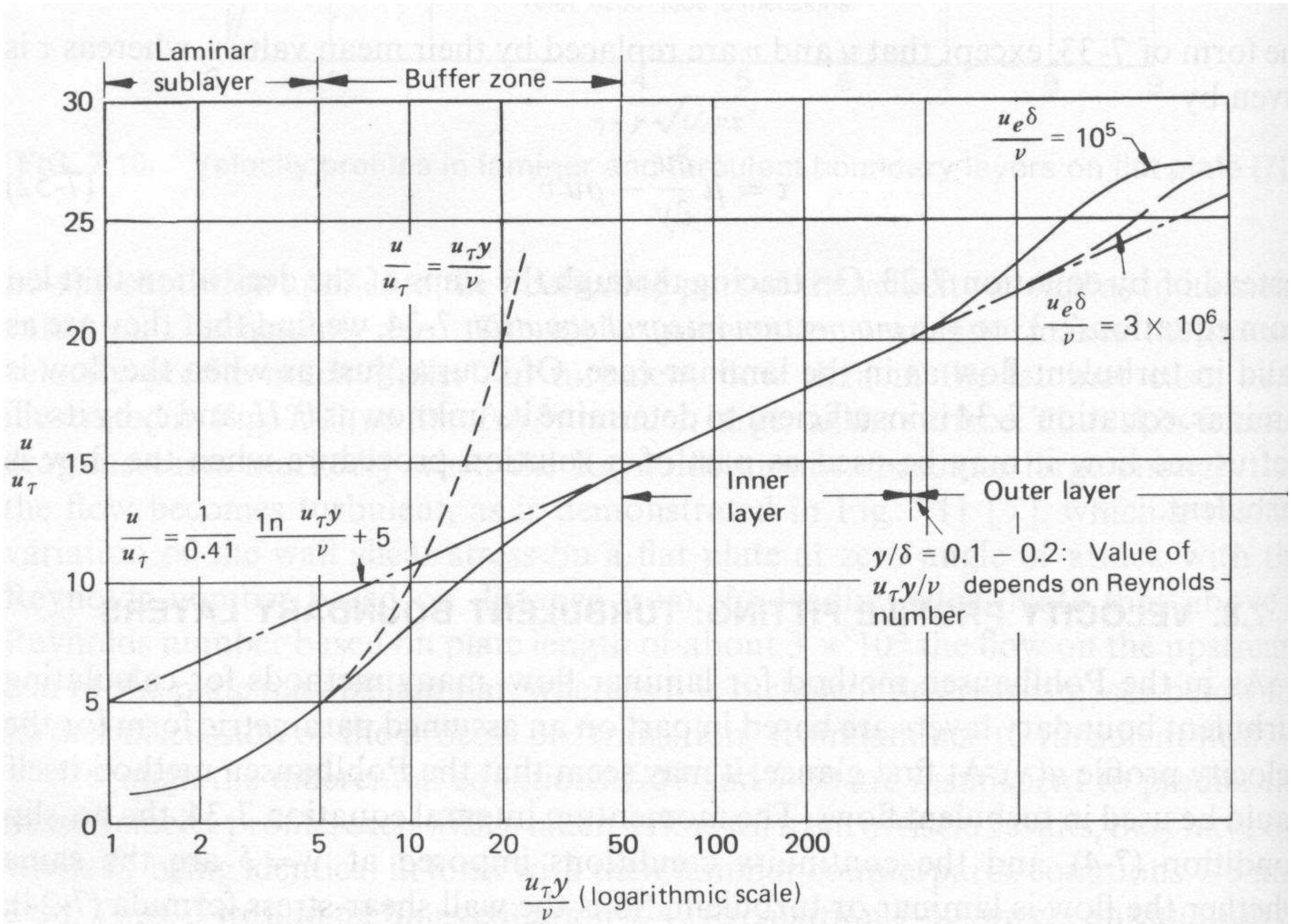

Figure 5: Regions in a Turbulent Boundary Layer

Characterization of the Turbulent Boundary Layer

The quantity u_τ that appears in the graph is called the friction velocity and is a quantity related to the wall shear stress that has units of velocity

$$u_\tau \equiv \sqrt{\frac{\tau_w}{\rho}}. \tag{7}$$

In the laminar sublayer, the shear stress is given by

$$\tau = \mu \frac{\partial u}{\partial y},$$

and it will not vary much from its value at the wall, τ_w, since the region is so thin. We can therefore integrate to get

$$\tau_w y = \mu u. \tag{8}$$

Introducing the friction velocity we have

$$u^+ \equiv \frac{u}{u_\tau} \approx \frac{\rho u_\tau y}{\mu} \equiv y^+, \tag{9}$$

which is a Reynolds number based on u_τ and the distance from the wall.

Outside the laminar sublayer, we must include the turbulent stress in the governing equations, and $\tau = \mu \frac{\partial u}{\partial y}$ will no longer work. In the inner layer we assume the flow to be so dominated by turbulent mixing, that it is essentially independent of the external flow. The only scale available for the mean velocity in the inner layer is

$$\sqrt{\frac{\tau}{\rho}},$$

which we take again to be nearly constant and equal to u_τ. The slope of the mean velocity profile is supposed to satisfy

$$\frac{\partial u}{\partial y} \approx \frac{u_\tau}{l},$$

where l is a characteristic length is usually called a *mixing length*. This mixing length is important in the development of algebraic turbulence models for boundary layers. Since the only length scale available is the distance from the wall

$$l = \kappa y,$$

where κ is a dimensionless constant and then

$$\frac{\partial u}{\partial y} \approx \frac{u_\tau}{\kappa y}, \tag{10}$$

which can be integrated to get

$$\frac{u}{u_\tau} = \frac{1}{\kappa} \ln y + C', \tag{11}$$

and by letting

$$C' = \frac{1}{\kappa} \ln \frac{\rho u_\tau}{\mu} + C,$$

we get the famous *law of the wall*

$$u^+ \equiv \frac{u}{u_\tau} = \frac{1}{\kappa} \ln y^+ + C, \tag{12}$$

which, for $C = 5.2$ and $\kappa = 0.41$ very accurately represents the velocity distribution in the inner layer.

In the outer layer, dimensional analysis leads to the *velocity defect law*

$$\frac{V_e - u}{u_\tau} = f\left(\frac{y}{\delta(x)}; x\right). \tag{13}$$

Coles found that the experimental data available (from a variety of sources) could be fit very well by letting f be the product of some function of x and another function of y/δ only. This was his *law of the wake* which leads to the formula

$$u^+ \equiv \frac{u}{u_\tau} = \frac{1}{\kappa}\ln y^+ + C + \frac{2}{\kappa}\Pi(x)\sin^2\frac{\pi y}{2\delta(x)} \quad \text{for } \; y \leq \delta(x), \tag{14}$$

which is very accurate outside the laminar sublayer, that is in both the inner and outer layers, for properly chosen Π, δ, and u_τ.

If we ignore the laminar sublayer, we can calculate θ and δ^* in terms of

Π, δ, and u_τ. Coles gives the formulas

$$\begin{aligned}\frac{\delta^*}{\delta} &= \frac{u_\tau}{\kappa V_e}(1+\Pi)\\ \frac{\theta}{\delta} &= \frac{\delta^*}{\delta} - \frac{2}{\kappa}\left(\frac{u_\tau}{V_e}\right)^2 \left\{1 + \Pi\left(1 + \frac{1}{\pi}S_i(\pi)\right) + \frac{3}{2}\Pi^2\right\},\end{aligned}$$

where

$$S_i(\pi) = \int_0^\pi \frac{\sin x}{x} dx \equiv 1.8516.$$

Evaluating Equation 14 at $y = \delta$, where $u = V_e$, gives a third equation

$$\frac{V_e}{u_\tau} = \frac{1}{\kappa}\ln\frac{\delta u_\tau}{\nu} + C + \frac{2}{\kappa}\Pi(x).$$

This results in five equations (counting the momentum integral equation) for the six unknowns θ, δ^*, c_f, Π, δ, and u_τ. What can we do? We need an extra equation which is usually derived from the *momentum-of-momentum* equation and leads to various methods for the integration of turbulent boundary layers and in particular Head's method.

Turbulent Flat-Plate Boundary Layer

Experimental measurements have shown that the time-averaged velocity may be represented by the power law

$$\frac{u}{V_e} = \left(\frac{y}{\delta}\right)^{\frac{1}{7}},$$

when the local Reynolds number, Re_x, is in the range 5×10^5 to 1×10^7. However, note that the velocity gradient for this profile

$$\frac{\partial u}{\partial y} = \frac{V_e}{7} \frac{1}{\delta^{\frac{1}{7}}} \frac{1}{y^{\frac{6}{7}}}$$

goes to infinity at the wall. We need another piece of experimental information: a correlation for the shear stress at the wall. Blausis found out that the skin friction coefficient for a turbulent boundary layer on a flat plate where the local Reynolds number, Re_x, is in the range 5×10^5 to 1×10^7 is given by

$$C_f = \frac{\tau}{1/2 \rho V_e^2} = 0.0456 \left(\frac{\nu}{V_e \delta} \right)^{0.25} .$$

The Von Karman integral momentum equation states that $\frac{d\theta}{dx} = \frac{1}{2} C_f$. By plugging in the expressions for C_f and $\frac{u}{V_e}$ that are found experimentally, one can show that

$$\frac{\delta}{x} = \frac{0.3747}{Re_x^{0.2}} \qquad (15)$$

Comparing the turbulent correlation given by this equation with the result that we obtained in laminar flows, we see that a turbulent boundary layer grows faster than a laminar one. Moreover, for the same free stream conditions, the turbulent boundary layer is significantly thicker than the laminar one.

Head's Method for Turbulent Boundary Layers

Head's method is based on the concept of an entrainment velocity. If $\delta(x)$ is the boundary layer thickness, the volume rate of flow within the boundary layer at x is

$$Q(x) = \int_0^{\delta(x)} u \, dy. \tag{16}$$

The entrainment velocity, E, is the rate at which Q increases with x

$$E = \frac{dQ}{dx}. \tag{17}$$

You can get an idea of what these concepts mean from the Figure below.

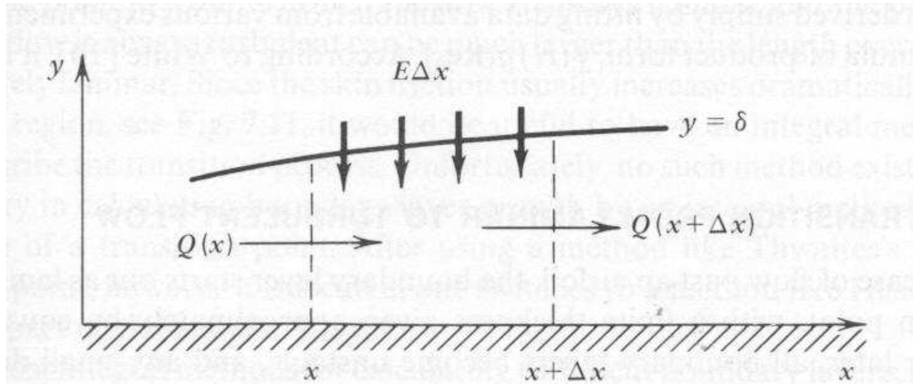

Figure 6: Entrainment Concept

Combining Equation 16 with the definition of displacement thickness we find that

$$\delta^* = \delta - \frac{Q}{V_e}.$$

Then

$$E = \frac{d}{dx} V_e(\delta - \delta^*),$$

which we can write

$$E = \frac{d}{dx}(V_e \theta H_1),$$

where

$$H_1 \equiv \frac{\delta - \delta^*}{\theta}.$$

Head assumed that the dimensionless entrainment velocity E/V_e depends only on H_1 and that H_1, in turn, is a function of $H \equiv \delta^*/\theta$. Cebeci and Bradshaw fit several sets of experimental data with the following formulas:

$$\frac{1}{V_e}\frac{d}{dx}(V_e \theta H_1) = 0.0306(H_1 - 3)^{-0.6169} \tag{18}$$

and

$$\begin{aligned} H_1 &= 3.3 + 0.8234(H - 1.1)^{-1.287} \quad \text{for } H \leq 1.6 \\ &= 3.3 + 1.5501(H - 0.6778)^{-3.064} \quad \text{for } H > 1.6. \end{aligned} \tag{19}$$

Together with the Von Karman integral momentum equation, Equations 18 and 19 represent three equations on four unknowns θ, H, H_1, and c_f. Head completes the set with the Ludwieg-Tillman skin friction law

$$c_f = 0.246 \times 10^{-0.678H} \mathsf{Re}_\theta^{-0.268}, \tag{20}$$

which was simply derived by fitting data available from various experimental studies with a formula of product form, $f(H)g(\mathsf{Re}_\theta)$, which is accurate to within 10%.

The solution procedure goes as follows. Given

$$\begin{aligned} \frac{d\theta}{dx} &= \frac{1}{2}c_f - \frac{\theta}{V_e}(2 + H) \\ \frac{1}{V_e}\frac{d}{dx}(V_e \theta H_1) &= 0.0306(H_1 - 3)^{-0.6169} \end{aligned} \tag{21}$$

we have two equations to march θ and H_1 downstream, given initial conditions. Once we have advanced θ and H_1 to the next station (with whatever procedure you choose - a Runge-Kutta method will do just fine) we can obtain H from the inverse of Equation 19

$$\begin{aligned} H &= 3.0 && \text{for } H_1 < 3.3 \\ H &= 0.6778 + 1.1536(H_1 - 3.3)^{-0.326} && \text{for } 3.3 < H_1 < 5.3 \\ H &= 1.1 + 0.86(H_1 - 3.3)^{-0.777} && \text{for } H_1 > 5.3 \end{aligned} \tag{22}$$

and using these values and the Ludwieg-Tillman Equation 20 we can obtain the skin friction coefficient, c_f. With all of this information we can characterize the boundary layer at that particular station and repeat the procedure to advance to the following station.